Supporting information

Electrospinning Hierarchical LiV_3O_8 Nanowire-in-Network for High-Rate and Long-Life Lithium Batteries

Wenhao Ren,‡ Zhiping Zheng,‡ Yanzhu Luo, Wei Chen,* Chaojiang Niu, Kangning Zhao, Mengyu Yan, Lei Zhang, Jiashen Meng, and Liqiang Mai*

State Key Laboratory of Advanced Technology for Materials Synthesis and Processing, Wuhan University of Technology, Hubei, Wuhan 430070, China
E-mail:mlq518@whut.edu.cn; chenwei_juan@sina.com
Fax: +86-27-87644867; Tel: +86-27-87467595

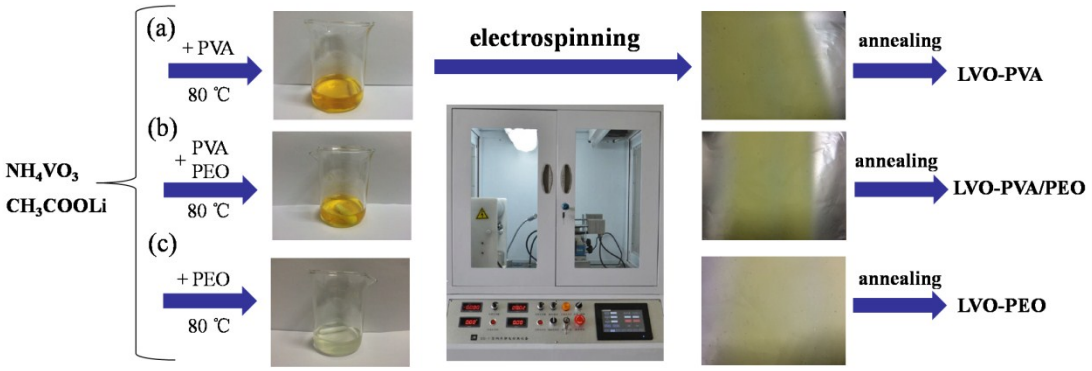

Fig. S1 Related photographs of the synthesis processes for the LVO-PVA (a), LVO-PVA/PEO (b) and LVO-PEO (c), respectively.

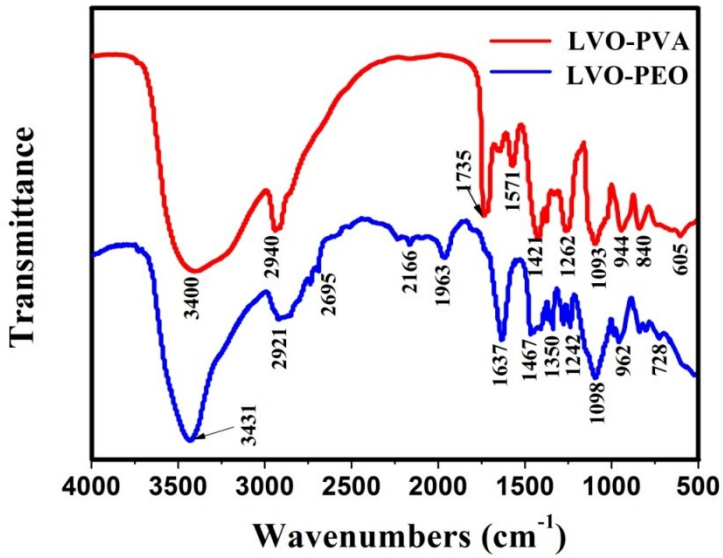

Fig. S2 FTIR spectra of electrospun LVO-PVA and LVO-PEO composite before annealing.

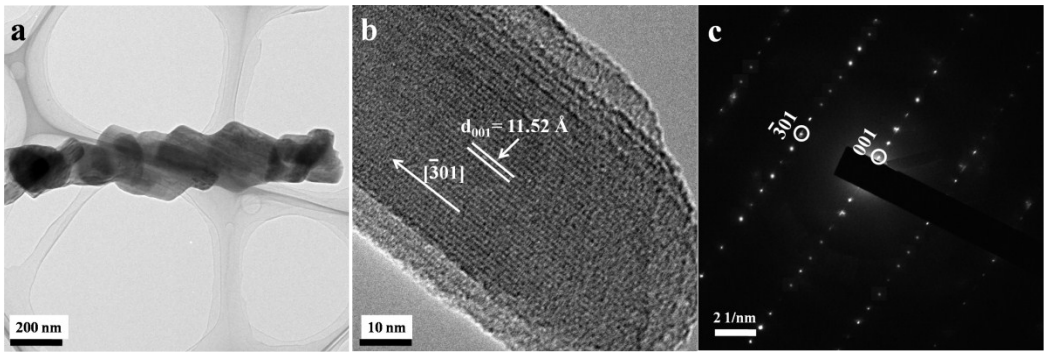

Fig. S3 TEM image (a), HRTEM image (b) and SAED patterns (c) of hierarchical LVO-PVA/PEO nanowire.

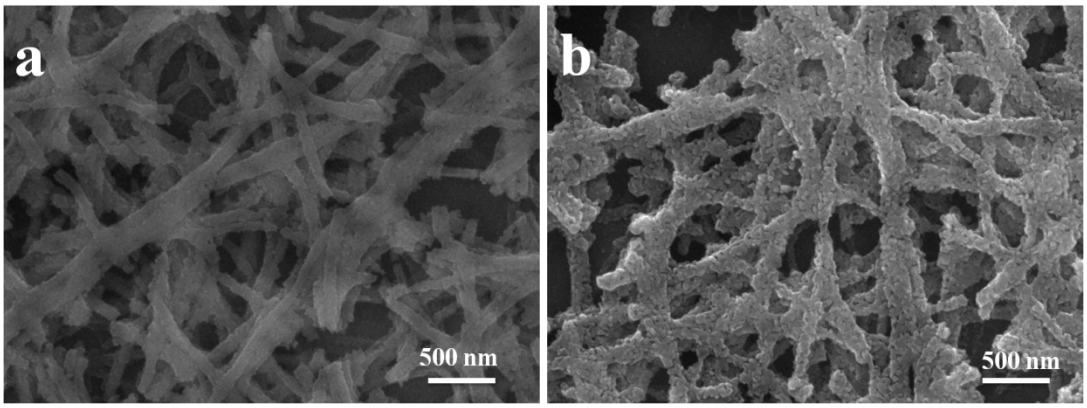

Fig. S4 SEM images of the electrospun LVO-PVA/PEO nanofibers after annealing at (a) 300 ºC and (b) 350 ºC for 2h. It indicates that the nucleary of original LiV_3O_8 grain and the decomposition of polymer components occur simultaneously so that hierarchical nanowires are formed.

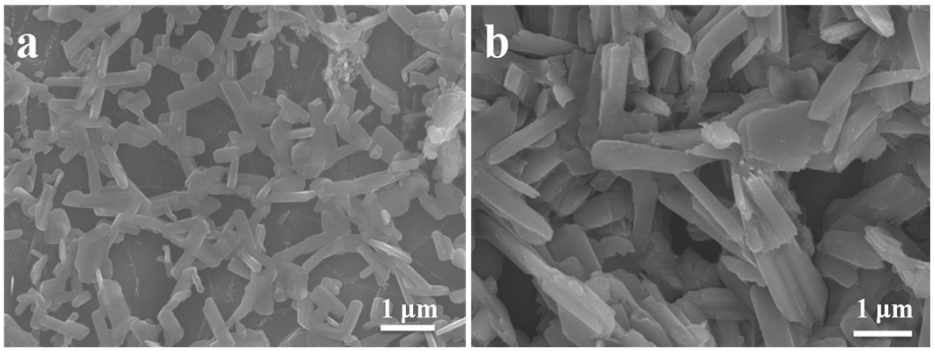

Fig. S5 SEM images of the electrospun LVO-PVA/PEO nanofibers after annealing at 450 ºC. The size of LiV_3O_8 nanorods grow much bigger and it consumes a large number of connected materials so that the hierarchical network structure cannot be maintained.

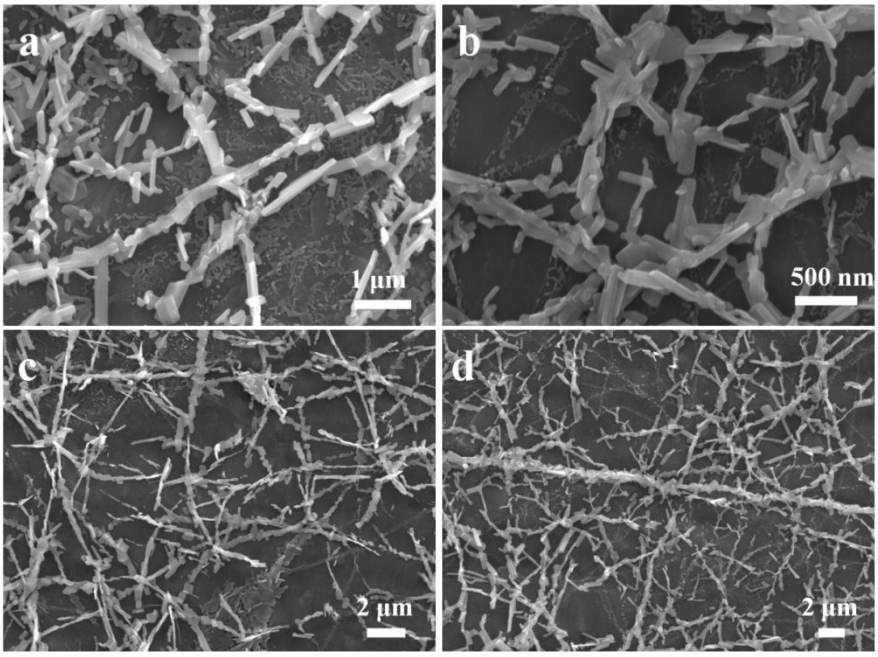

Fig. S6 FESEM images of the electrospun LVO-PVA/PEO nanofibers after annealing at 400 ℃. The weight ratio of PVA and PEO is 3:1 (a), 2:1 (b), 1:2 (c) and 1:3 (d) for the starting materials.

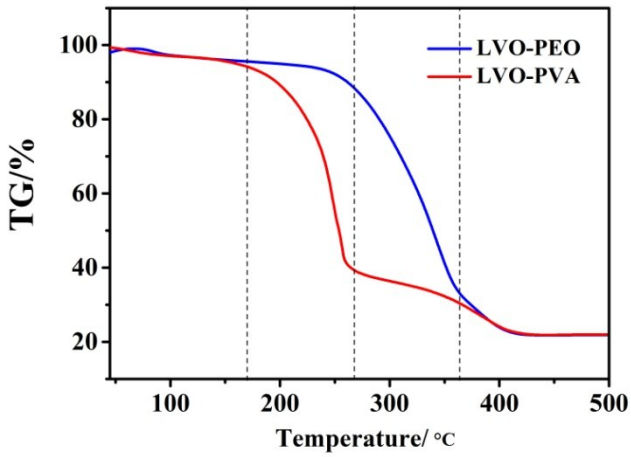

Fig. S7 TG images of the electrospun LVO-PVA and LVO-PEO nanofibers.

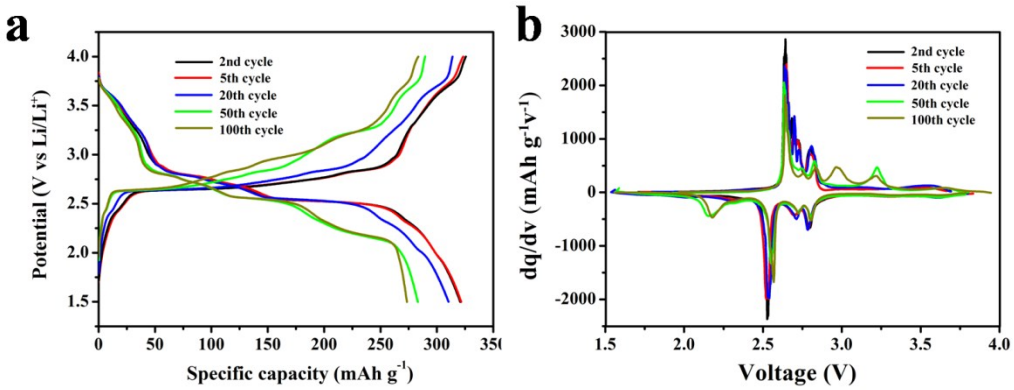

Fig. S8 Charge–discharge curves (a) and differential capacity *vs*. voltage curves (b) of LVO-PVA/PEO sample at different cycles.

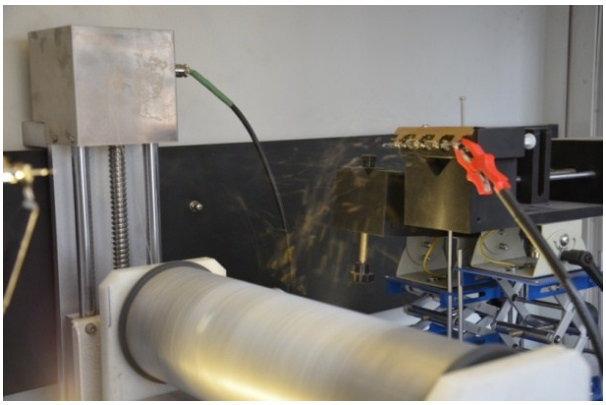

Fig. S9 Electrospinning process with four working injectors

Table S1. Comparison of the electrochemical performance of LiV_3O_8 based cathode materials for lithium batteries.

	Material	Current density (mA g^{-1})	Maximum capacity (mAh g^{-1})	Cycle numbers	Capacity after cycle (mAh g^{-1})	Decay per cycle (%)	Reference
		100	320	100	272	0.153	
1	LiV_3O_8	1000	254	500	129	0.098	Our work
		2000	202	500	103	0.099	
2	Mo- LiV_3O_8	300	269	100	206	0.235	S1
3	$Li_xV_2O_5/LiV_3O_8$	300	195	420	161	0.042	S2
4	G-LiV_3O_8	300	226	100	197	0.129	S3
5	LiV_3O_8	1000	240	100	194	0.190	S4
6	LiV_3O_8	300	200	200	191	0.023	S5
7	LiV_3O_8/PTh	300	250	50	217	0.264	S6

Reference

S1. H. Song, Y. Liu, C. Zhang, C. Liu and G. Cao, *J. Mater. Chem. A*, 2015, **3**, 3547-3558.

S2. D. Sun, G. Jin, H. Wang, X. Huang, Y. Ren, J. Jiang, H. He and Y. Tang, *J. Mater. Chem. A*, 2014, **2**, 8009-8016.

S3. R. Mo, Y. Du, N. Zhang, D. Rooney and K. Sun, *Chem. Commun.*, 2013, **49**, 9143-9145.

S4. S. H. Choi and Y. C. Kang, *Chem. Eur. J.*, 2013, **19**, 17305-17309.

S5. R. Mo, Y. Du, N. Zhang, D. Rooney and K. Sun, *J. Power Sources*, 2014, **257**, 319-324.

S6. H. Guo, L. Liu, H. Shu, X. Yang, Z. Yang, M. Zhou, J. Tan, Z. Yan, H. Hu and X. Wang, *J. Power Sources*, 2014, **247**, 117–126.